

SOME RESULTS CONCERNING NO-STORAGE WIND-DIESEL SYSTEMS CONTROL

Ciprian VLAD¹, Nicolaos Antonio CUTULULIS², Julie LEFEBVRE³, Emil CEANGA¹

¹*"Dunărea de Jos" University of Galați, Electrical and Electronics Engineering Faculty, Stiinței, no. 2, 8000146 – Galați, Romania,*

²*Risø National Laboratory, Roskilde, Denmark,*

³*Université du Québec à Rimouski, Canada.*

Abstract: This paper deal with the dynamics of an autonomous no storage wind-diesel system, comprising a diesel generator and a controlled wind system with a hypo/hyper synchronous cascade. The objective is to maximize the wind energy penetration rate, by an optimization control system, respecting the quality standard concerning the frequency deviation in the AC local grid. Also, the influence of the diesel drive train on the system's dynamics performances is discussed.

Keywords: Wind energy, Wind-diesel system, Wind energy penetration rate, Optimization control system, Frequency deviation.

1. INTRODUCTION

The advent of electrical power made possible a centralized generation of power, and the interconnection of electricity grids led to the firm and robust power supply systems that most of us enjoy today. However, there are still large parts of the world which do not benefit from this development.

In order to assure an uninterrupted energy supply, in autonomous wind power systems there are other electrical energy sources: diesel generators, batteries and/or photovoltaic panels. A wind power system along with any of these sources (standard or renewable) forms the so-called Hybrid Wind Power Systems (HWPS) (Hunter and Elliot, 1994).

The problems regarding the control of the HWPS are more complex compared to grid-connected wind power systems. The main problem is the major discrepancy between the stochastic and strongly fluctuating power from the wind (wind speed is a random, strongly non-stationary process, with turbulence and extreme variations) and the extremely exigent control demands regarding the electrical energy parameters (frequency, voltage, etc.) (Cutululis, 2005; Baring-Gould, *et al.*, 2004).

There are different HWPS structures:

- wind-diesel system with no energy storage (Jeffries, *et al.*, 1996);
- wind-diesel system with kinetics energy storage (flywheel);
- wind-diesel system with long-term energy storage (batteries), with or without photovoltaic sources, etc.

The main criteria in choosing HWPS structure are:

- satisfying the quality demands of electrical energy parameters (frequency, voltage, etc.);
- minimizing the electrical energy production costs in autonomous systems. This involves a small price of investment and a highest average of wind energy penetration rate.

In the classical structure of wind-diesel system with no energy storage, the induction generator driven by wind turbine is directly coupled to the AC grid together with the synchronous generator of the diesel generator (Lundsager and Bindner, 1994). This solution is very economic in terms of investment costs (no needs for static converters and control systems), but it has a lower penetration rate, due to:

- the frequency variations in the AC local grid can became too large when the wind power generation

rate increases (Lundsager, *et al.*, 2001);
- the wind power system is not working in an optimal conversion regime.

Lately, HWPS structures with internal DC bus, connected to the AC bus through an inverter, are used. Both induction and synchronous generators are coupled at DC bus through rectifiers along with other DC sources: batteries, for long term energy storage, coupled through bidirectional chopper, photovoltaic sources, etc. This kind of structure can assure a high average wind energy penetration rate, in optimal regime of energetic conversion, but with big investment costs due to the extensive use of static converters (Lundsager, *et al.*, 2001).

This paper deals with HWPS structure without storage and with low cost of power electronics, which is able to assure optimal energetic conversion. The diesel generator and the wind system are connected directly to the AC bus. The wind system has a frequency controlled induction generator (hypo/hyper synchronous cascade) which assures optimal energetic conversion.

The approach adopted in this paper has the next premises:

- utilization of an accurate HWPS model in low frequencies band. The rapid dynamics of electrical subsystems are neglected because the special interest concerns the automatic speed control (ASC) performances of the diesel generator (the dynamic of this loop determines frequency deviations in the local grid);

- the ASC loop is excited by wind system power fluctuation. The average wind speed growth determines the improvement of the wind energy penetration rate, by reducing the diesel load (assuming a constant grid load). In the same time, the wind power fluctuation will increase due to the direct relation between the variance of the wind speed turbulence component and the wind speed average value. In these conditions, it is not a trivial task to ensure the performances of the ASC loop dynamics in order to respect the quality standards of frequency deviations;

- the optimal conversion loop's control variable is the electromagnetic torque of the induction generator. When the wind energetic level and the turbulence component magnitude are high, the variations of the electromagnetic torque, induced by the control loop, produce disturbances in the ASC of the diesel generator. The level of those disturbances depends on the control algorithm properties. A control loop which acts „strongly” regarding the optimization objective will generate important disturbances in the ASC loop. Then, it's obvious the dilemma: “wind energy penetration rate against frequency deviation in local grid”. In this context, some contributions regarding properties of the HWPS structure without energy storage are presented.

The paper is structured as follows: the analyzed HWPS structure and quality demands for the electrical energy parameters (frequency, voltage) are presented in next section. Section 3 is dedicated to modeling of the wind-diesel system and to the wind speed simulation. The numerical simulation results regarding HWPS performances are presented in Section 4. Finally, some concluding remarks end this paper.

2. SYSTEM STRUCTURES AND TECHNICAL DEMANDS

The considered HWPS structure is presented in Fig. 1. The diesel motor is controlled through the ASC loop, which is excited by shaft torque variations due to the active power variations in the local grid or/and induced by the wind power system. HWPS has a control system which assures the maximization of wind turbine power coefficient, $C_p(\lambda)$. Consider the optimal tip speed ratio λ_{opt} which correspond to maximum power coefficient $C_p(\lambda)$. The control system that assure wind energy optimal conversion is a tracking loop which brings the turbine rotational speed $\Omega(t)$ at the optimal value:

$$(1) \quad \Omega_{opt}(t) = \frac{\lambda_{opt}}{R} \cdot v(t)$$

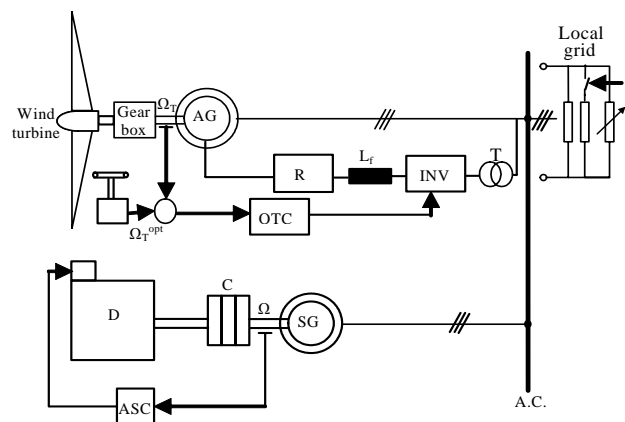


Fig.1. HWPS system (AG-asynchronous generator, R-rectifier, INV-inverter, OTC-optimization tracking loop controller, T-transformer, D-diesel-generator, SG-synchronous generator, C-clutch)

The tracking loop controller acts on the electro mechanic characteristic of the induction generator through a hypo or hyper synchronous cascade. The optimization tracking loop controller (OTC) acts on the inverter and adjusts the synchronous speed (displacement of the intersection point between the generator's electro mechanic characteristic and the abscissa). Tracking loop function is to control the electromagnetic torque for modifying diesel variations. These variations excite the control loops from diesel generator level. Fast wind speed

variations, due to turbulences and gusts, can cause important frequency and voltage deviations in local grid.

The maximum allowed frequency deviation depends on its time length and on the voltage deviation. This dependency is shown in Fig. 2. As it can be observed, the frequency deviation demands are stricter than the voltage ones. Hence, the priority was given on ASC loop dynamic performances, for different wind speeds.

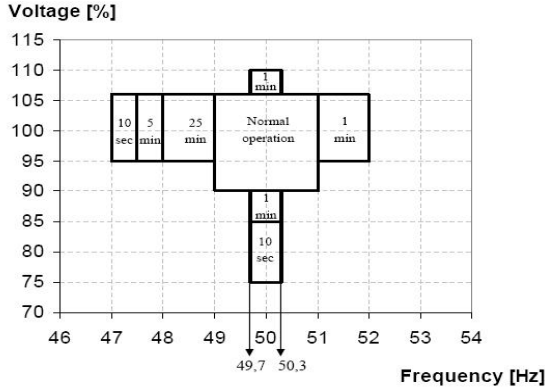


Fig.2. Voltage and frequency allowable deviations (Danish Technical Regulation TF 3.2.6, 2004)

3. SYSTEM MODELING

3.1. Diesel Generator Modeling

The diesel model is structured on two subsystems: fuel supply and combustion subsystem, and the mechanical subsystem. The first subsystem has as input the set point for the fuel flow rate (q_d), and as output the average shaft torque (T_{da}). The mathematical model for the first subsystem (Burton, *et al.*, 2001) is:

$$(2) \quad q_{eff} = \frac{e^{-\tau_d s}}{1 + \tau_c s} q_d$$

$$(3) \quad p_e = \varepsilon K_c q_{eff}$$

$$(4) \quad T_{da} = K_v (p_e - p_0)$$

where:

q_{eff} - the effective fuel flow rate [p.u.]; τ_d - the time delay of combustion [s]; τ_c - a time constant representing the actuator and combustion process dynamic [s]; p_e - the average engine chamber pressure [p.u.]; ε - the fuel efficiency [p.u.]; K_c - a constant relating pressure and fuel consumption [p.u.]; K_v - the stoke volume of the engine [p.u.]; p_0 - the zero torque pressure [p.u.].

Mechanical subsystem is presented in Fig. 3, with: J_d , J_s , J_{fc} , J_{fw} - the inertia of the diesel engine, electrical generator, flywheel and clutch, and the generator's

flywheel, respectively; C_{cl} , D_{cl} - the torsional stiffness and damping of the coupling, respectively; T_s the torque from the electrical generator.

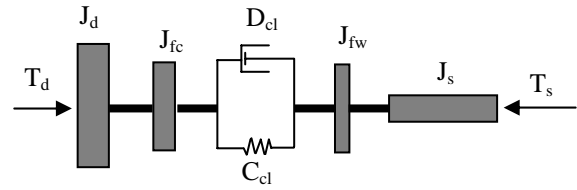


Fig.3. Diesel drive model (Uhlen, 1994)

The equations describing this subsystem are:

$$(5) \quad \dot{\theta}_{cl} = \omega_d - \omega_s$$

$$(6) \quad (J_d + J_{fc}) \dot{\omega}_d = T_d - (D_d + D_{fc}) \omega_d - T_{cl}$$

$$(7) \quad (J_{fw} + J_s) \dot{\omega}_s = T_{cl} - (D_{fw} + D_s) \omega_s - T_s$$

where:

$$(8) \quad T_{cl} = C_{cl} \theta_{cl} + D_{cl} \dot{\theta}_{cl}$$

θ_{cl} is the torsion angle between the engine and the generator shaft [p.u.]; ω_d - the rotational speed of the diesel engine [p.u.]; ω_s - the rotational speed of the electrical generator [p.u.]; D_d , D_s , D_{fc} , D_{fw} - the frictional damping of the diesel engine, the electrical generator, the flywheel and clutch, and the generator's flywheel, respectively; T_{cl} - the torque from the generator [p.u.].

The diesel governor (ASC) controls the fuel flow in order to maintain a desired rotational speed of the diesel engine. Fig. 4 shows the electronic PID governor model, where T_m is the dynamics of the speed transducer, ω_{ref} is the engine speed set point and δ is the governor droop.

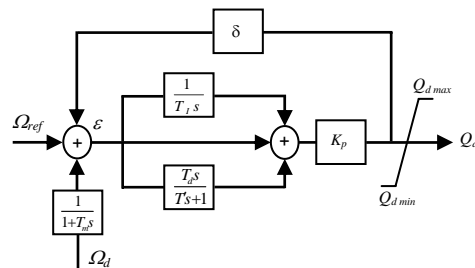


Fig.4. The diesel electronic governor model

The diesel generator has 60kVA nominal power and a PID controller for the ASC loop.

3.2. Wind System Modeling

The aerodynamic power is:

$$(9) \quad P_w = \frac{1}{2} C_p \rho A_r v_w^2$$

where: $C_p(\lambda)$ – power efficiency coefficient; ρ - air density [kg/m^3]; A_r – rotor swept area [m^2]; v_w – single point wind speed in the axial direction [m/s]; λ – tip speed ratio:

$$(10) \quad \lambda = \frac{\omega_t R}{v_w}$$

with ω_t and R - rotational speed of wind turbine and blade length, respectively. The mechanical rotor torque (T_w) is given by:

$$(11) \quad T_w = \frac{P_w}{\omega_t} = \frac{1}{2} C_p \rho A_r \frac{v_w^3}{\omega_t}$$

The mechanical system is considered in two variants: rigid drive train, and flexible drive train. In the first case, the dynamic equation of the drive train is:

$$(12) \quad \dot{\omega}_t = \frac{1}{J_t} (T_w - n T_{ga})$$

where T_{ga} is the induction generator torque and n is the gear ratio. In the second case, the dynamic equations are:

$$(13) \quad \begin{aligned} \dot{\theta}_c &= \omega - \frac{1}{n} \omega_a \\ \dot{\omega} &= \frac{1}{J_t} \left(\frac{1}{2} C_p \rho A_r \frac{v_w^3}{\omega} - C_c \theta_c - (D_t + D_c) \omega + \frac{D_c}{n} \omega_a \right) \\ \dot{\omega}_a &= \frac{1}{J_a + \frac{1}{n^2} J_g} \left(\frac{C_c}{n} \theta_c + \frac{D_c}{n} \omega - \left(D_a + \frac{D_c + D_g}{n^2} \right) \omega_a - T_{ga} \right) \end{aligned}$$

where: θ_c – relative axial displacement between wind hub and gear [p.u.]; ω_a – rotational speed of induction generator [p.u.]; J_t , J_a and J_g – inertia moments of wind turbine, induction generator and gear [s]; C_c – torsional stiffness constant of flexible coupling [p.u.]; D_t , D_c , D_a , and D_g - the frictional damping constant of the wind turbine, flexible coupling, electrical generator and gear, respectively [p.u.]. Induction generator torque T_{ga} is controlled by the OTC.

Wind turbine has 60kVA nominal power. The power coefficient characteristic is obtained by a six order polynomial regression:

$$(14) \quad C_p(\lambda) = \sum_{i=1}^n a_i \lambda^i$$

Wind power, $P_w(v, \omega_t)$, characteristics are presented in Fig. 5, along with the optimal regime characteristic (ORC). Wind torque characteristics are presented in Fig. 6, along with the induction generator electromechanical characteristics. When hypo or

hyper synchronous cascade is used, the induction generator electromechanical characteristic modifies its operational points (I curves in Fig 6). In numerical simulation a linear form of the electromechanical characteristic, in the working area, was used.

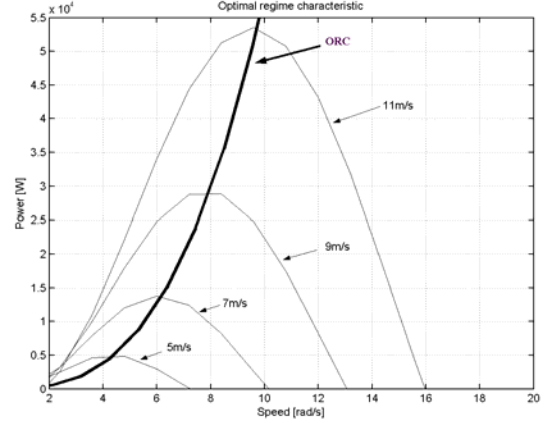


Fig.5. Wind optimal power characteristic

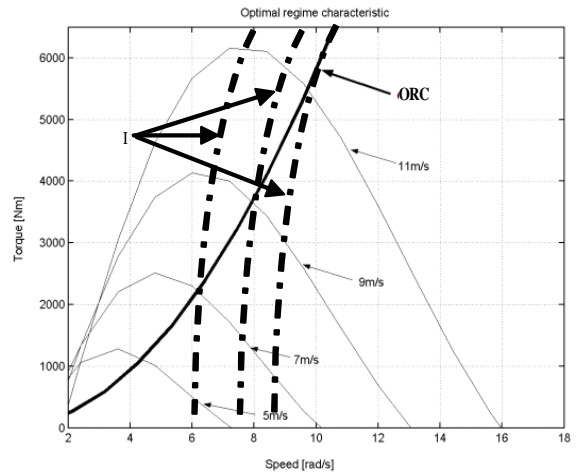


Fig.6. Wind and generated torque characteristic

3.3. Wind Speed Modeling

The wind speed $v(t)$ is considered on the form: $v(t) = \bar{v}(t) + v_t(t)$, where $\bar{v}(t)$ is the medium and long-term component and $v_t(t)$ the turbulence component. For the time scale corresponding to the turbulence component, one considers that \bar{v} is the mean wind speed taking as a constant. The turbulence field properties depend on the mean wind speed, \bar{v} , by means of (Burton, *et al.*, 2001): turbulence intensity, $I = \sigma / \bar{v}$, where σ is the standard deviation of the turbulence component; turbulence length scale, L .

The structure for numerical generation of $v_t(t)$, with the von Karman model used for the turbulence component (Nichita, *et al.*, 2002; Welfonder), is presented in Fig. 7.

HWPS numerical simulation analysis was conducted with a simplified model of turbulence component, wherein the non-integer degree filter was replaced by a first degree filter with $T_f = 20s$. The static gain was adopted so the standard deviation of the z variable at the filter output has unit value.

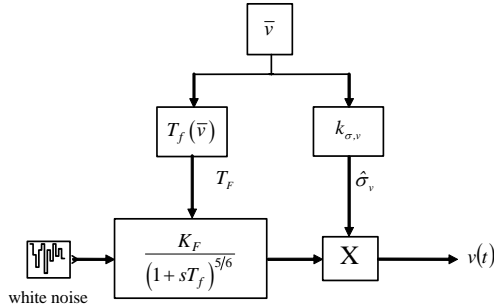


Fig.7. Turbulence component generation schema

The results presented in Fig. 8 correspond to the case when turbulence intensity is $I = 0.17$. Two wind profiles, for $\bar{v} = 8$ m/s and $\bar{v} = 5$ m/s, are presented in Fig. 8.

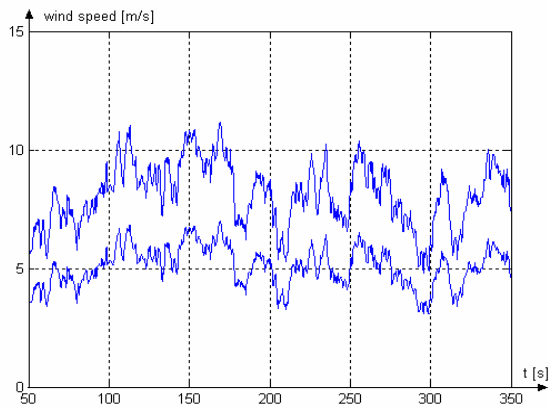


Fig.8. Modeled wind profiles used in simulation studies

4. SIMULATION RESULTS

4.1. Dynamic performances of the ASC

Two structures of the diesel mechanical subsystem with and without flexible coupling have been analyzed.

Fig. 9 presents the dynamics of the ASC for a step variation of the load torque (ω_{ω_F} and ω_{ω_D} represent the responses in case of flexible coupling and direct coupling). A worst behavior can be noticed when the flexible coupling is used in order to decrease the mechanical stress. Therefore, two solutions are proposed for the autonomous wind-diesel coupling. One solution is to use the direct coupling between the diesel and the synchronous generator and the second one uses stiff elastic coupling (big values of the C_{cl} and D_{cl} parameters).

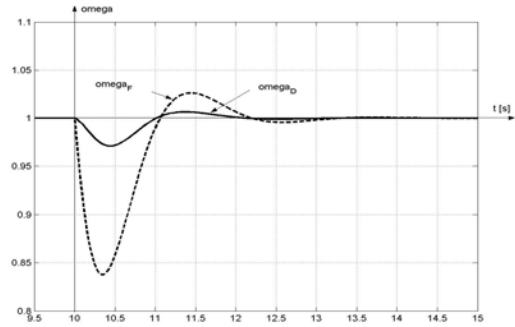


Fig.9. Flexible and direct coupling behaviors

4.2. Results concerning the optimal tracking controller

One main scope of the analysis performed through numerical simulation was to determine to which extent the parameters tuning can lead to a simultaneously control of the quality demand regarding allowable standard frequency deviations and maintain the operation point around the ORC.

In order to do that, the parameters that were analyzed are: local grid frequency deviations, tip speed ratio λ , power efficiency coefficient $C_p(\lambda)$ and supplied energy over a fixed period of time (300s).

If the tracking loop controller parameters are tuned strictly to maintain the tip speed ratio at optimal value $\lambda_{opt} = 6$ (i.e. power efficiency coefficient C_p is brought to maximal value), then the power efficiency coefficient evolution for $\bar{v} = 8$ m/s is illustrated in Fig. 10. In this case, the electromagnetic torque deviations are high and therefore, the induced perturbations in ASC loop determine deviations of frequency in the local grid well outside the allowable band. In order to limit those deviations to the allowable band, the tracking loop control demands were relaxed.

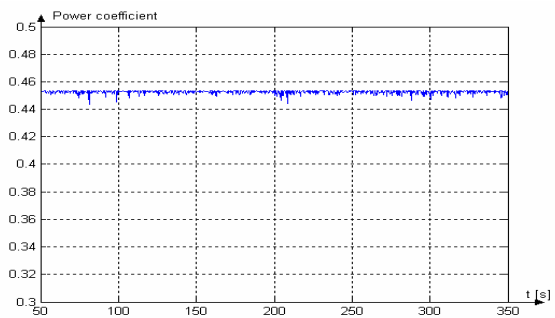


Fig.10. Power efficiency coefficient evolution

Next, there are presented the results from 3 operating modes considered:

1. tracking loop controller is tuned so that the frequency deviations for $\bar{v} = 8$ m/s are inside the allowable band;

2. static gain of the controller is 5 times smaller than in the previous case;
3. tracking loop is removed and the electrical generator operates according its natural characteristic.

The results can be observed in Fig. 12, 13, 14 and 15, where the above mentioned cases are represented by solid, dot and dash line, respectively. The produced energy (Fig. 11) shows that the energetic criterion in the tracking loop controller's tuning is not very important. If we compare it with tracking loop performances in the case 1 (Fig. 10), the supplied energy reduction in case 2 is only 2.5% (see also Fig. 11).

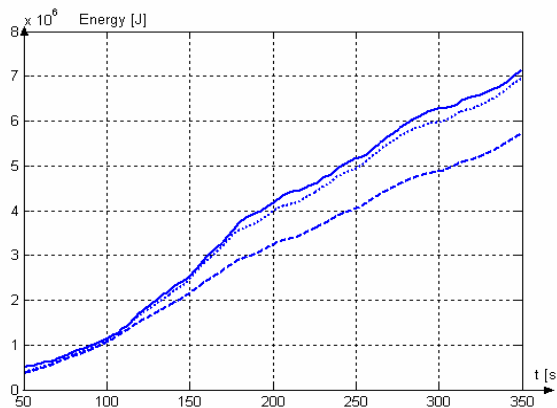


Fig.11. Supplied energy evolutions

Fig. 12 and 13 illustrate the evolutions of tip speed ratio and power efficiency coefficient. In the second case, the produced energy reduction is not significant, but the frequency deviations are substantially decreased (see Fig. 14).

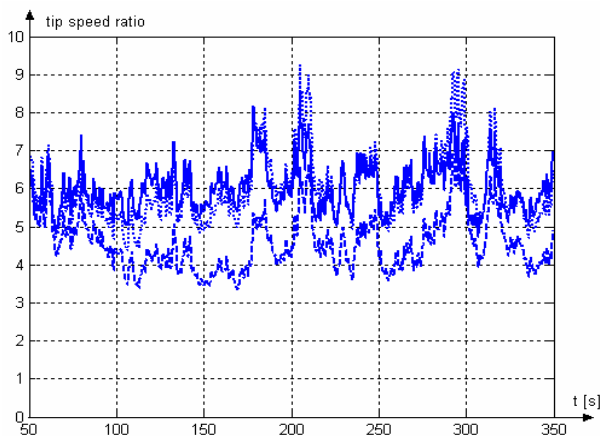


Fig.12. Tip speed ratio evolution

If the electrical generator operates in its natural characteristic (third case) then the produced energy reduction is around 22% (assuming a correct position of these characteristic), but the frequency deviations are very low (see Fig. 14).

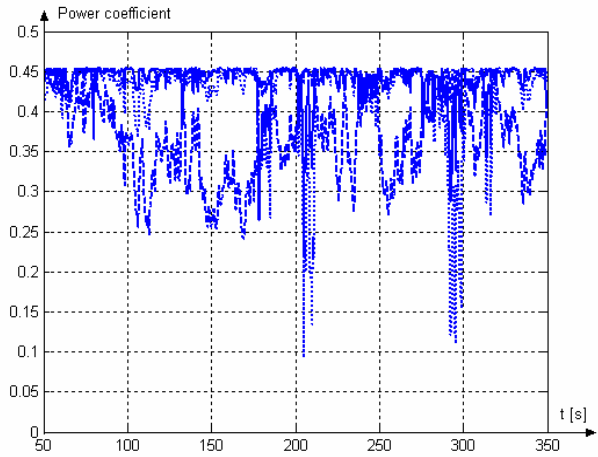


Fig.13. Power efficiency coefficient evolution

If the electrical generator operates in its natural characteristic (third case) then the produced energy reduction is around 22% (assuming a correct position of these characteristic), but the frequency deviations are very low (see Fig. 14).

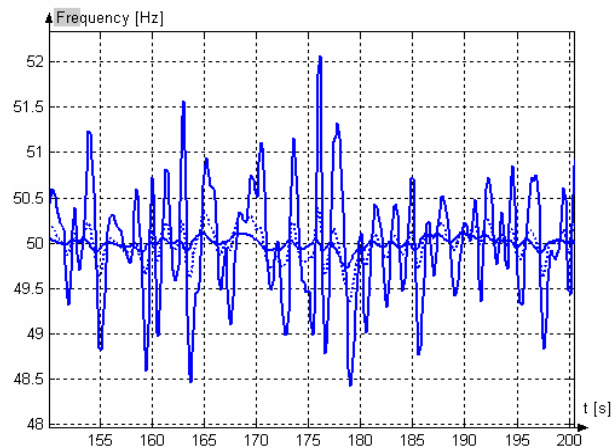


Fig.14. Grid frequency evolution

For low average wind speed, $\bar{v} = 5$ m/s, the controller tuned strictly for energy conversion optimization (case 1) induces smaller frequency deviations (see Fig. 17, thick curve is for $\bar{v} = 8$ m/s).

The explanation of these results can be obtained by examining simultaneously the evolutions of the induction generator torque T_{ga} and wind torque T_w . If the electrical generator operate in its natural characteristic (case 3), then the torques T_{ga} and T_w have similar evolutions (see Fig. 16).

When the tracking loop controller is tuned strictly for energy conversion optimization, it generates a «strong» evolution of T_{ga} torque (Fig. 15).

For wind speed regimes of $\bar{v} = 5$ m/s and $\bar{v} = 8$ m/s, the wind energy average penetration is: 10.4% and 42.3% respectively. If tracking loop is removed, for $\bar{v} = 8$ m/s, the penetration rate decrease to 34.5%.

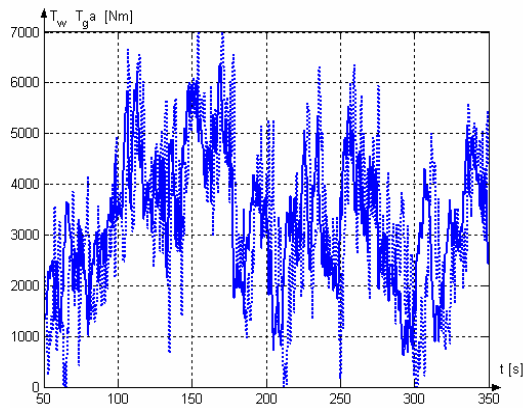


Fig.15. First case T_w and T_{ga} torque evolution

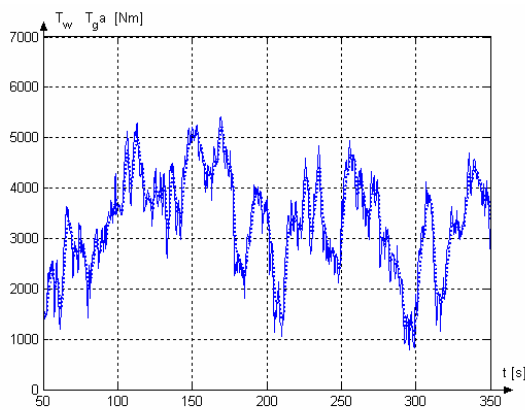


Fig.16. Third case T_w and T_{ga} torque evolution

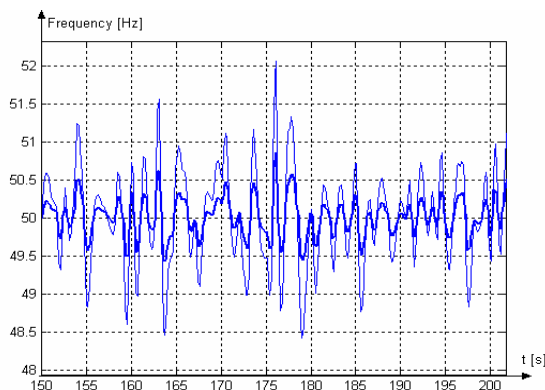


Fig.17. Grid frequency evolution ($\bar{v}=5$ and 8 m/s)

5. CONCLUSIONS

From the obtained results, we can conclude that in case of autonomous wind-diesel system it is better to use the direct coupling between the diesel and the synchronous generator or to use stiff elastic coupling (big values of the C_{cl} and D_{cl} parameters).

In order to achieve a high wind energy penetration rate, the wind power system should operate with wind speeds near to the nominal speed and the energy conversion should be optimized by means of a tracking control loop. In this case, for the HWPS

design it is essential to solve the dilemma: „wind energy penetration rate against frequency quality standard deviation”. The principle of solution for this dilemma is to adopt some relaxed demands concerning the ORC’s performances, because the energetic criteria in the tracking loop controller’s tuning is not very important.

6. REFERENCES

- Hunter, R., Elliot, G., (1994), *Wind-Diesel systems*, Cambridge University Press.
- Cutululis, N-A., (2005), *Contribuții privind sinteza strategiilor de conducere automată în sistemele de conversie a energiilor neconvenționale cu structuri hibride*, PhD Thesis, «Dunărea de Jos» University of Galați.
- Baring-Gould, I., Flowers, L., Lundsager, P., Mott, L., Shirazi, M., Zimmermann, J., (2004), *Worldwide Status of Wind – Diesel Applications*, DOE/AWEA/ CanWEA Wind – Diesel Workshop.
- Jeffries, W.Q., McGowan, J.G., Manwell, J.F., (1996), *Development of a dynamic model for no storage wind/diesel systems*. Wind Engineering, Vol. 20, No. 1, pp. 27-38.
- Lundsager, P., Bindner, H., (1994), *A simple, robust & reliable wind diesel concept for remote power supply*. Renewable Energy, Vol. 5, Part I, pp. 626-630.
- Lundsager, P., Bindner, H., Clausen, N.E., Frandsen, S., Hansen and L.H., Hansen, J.C., (June 2001), *Isolated Systems with Wind Power*. Main report. Risø National Laboratory, Roskilde.
- Danish Technical Regulation TF 3.2.6, (2004) *Wind turbines connected to grids with voltage below 100 kV – Technical regulation for the properties and the control of wind turbines* Doc. No. 177899.
- Uhlen, K., (1994), *Modelling and Robust Control of Autonomous Hybrid Power Systems*, PhD Thesis, Trondheim University.
- Burton, T., D. Sharpe, N. Jenkins and E. Bossanyi, (2001), *Wind Energy Handbook*, John Wiley & Sons.
- Nichita, C., Luca, D., Dakyo, B., Ceanga, E., (2002), *Large Band Simulation of the Wind Speed for Real Time Wind Turbine Simulators*, IEEE Transactions on Energy Conversion, Vol.17, No.4.
- Welfonder, E., Neifer, R. and Spanner, M. *Development and Experimental Identification of Dynamic Models for Wind Turbines*, Control Engineering Practice, Vol. 5, No. 1, pp. 63 – 73.